Flextensional fiber Bragg grating-based accelerometer for low frequency vibration measurement

Jinghua Zhang (张敬花)*, Xueguang Qiao (乔学光), Manli Hu (忽满利), Zhongyao Feng (冯忠耀), Hong Gao (高 宏), Yang Yang (杨 扬), and Rui Zhou (周 锐)

Department of Physics, Northwest University of China , Xi'an 710069, China

**Corresponding author: 1982zhangjinghua@163.com*

Received February 14, 2011; accepted April 21, 2011; posted online July 11, 2011

The intelligent structural health monitoring method, which uses a fiber Bragg grating (FBG) sensor, is a new approach in the field of civil engineering. However, it lacks a reliable FBG-based accelerometer for taking structural low frequency vibration measurements. In this letter, a flextensional FBG-based accelerometer is proposed and demonstrated. The experimental results indicate that the natural frequency of the developed accelerometer is 16.7 Hz, with a high sensitivity of 410.7 pm/g. In addition, it has a broad and flat response over low frequencies ranging from 1 to 10 Hz. The natural frequency and sensitivity of the accelerometer can be tuned by adding mass to tailor the sensor performance to specific applications. Experimental results are presented to demonstrate the good performance of the proposed FBG-based accelerometer. These results show that the proposed accelerometer is satisfactory for low frequency vibration measurements.

OCIS codes: 060.2370, 230.1480, 050.2770.
doi: 10.3788/COL201109.090607.

Vibrations widely exist in nature[1−4]. The proposed accelerometer in this letter mainly aims at conducting low frequency (below 10 Hz) vibration monitoring of large structures. For instance, the inherent frequencies of normal highway bridges and railway bridges range of 2–10 Hz. At present, piezoelectric electromagnetism class accelerometers are mainly used for measuring low frequency vibrations. However, the application of this type of sensor is limited because of natural insufficiencies[5,6], such as interference from electromagnetism and corrosion. In comparison, a fiber Bragg grating (FBG) sensor does not suffer from electromagnetic interference, it can be connected easily to a network, and is capable of taking highly precise measurements. Thus, it is very fit for monitoring low frequency vibrations.

In this letter, a flextensional FBG-based accelerometer is designed and manufactured. The sensing system is based on a flextensional member and has high sensitivity for acceleration measurements at low frequency ranges (below 10 Hz). The dynamic vibration measurements show that it is a good candidate for the measurement of low frequency vibrations below 10 Hz.

The FBG with a length of 10 mm was written in a photosensitive single mode optical fiber; it served as the sensing element in the proposed accelerometer. The FBG was mounted on the outboard of a flexible beam. With this setting, the light intensity reflected by the grating was modulated in accordance with the vibration of the flexible beam. The accelerometer is shown schematically in Fig. 1. Figure 2 shows the expansion graph of the elastic element (flextensional member), in which the elastic beam is uniformly distributed. The sensing grating was attached to the middle of the elastic beam, controlling the uniformity of the glue thickness. The elastic beam was fixed by the spacer according to the angle of bending. Figure 3 shows the schematic diagram of the spacer.

The mechanism consisted of a cylindrical concentration inertial mass, which was supported by a flextensional member. The mechanical stop was designed to prevent the sensor from being broken and to ensure that the FBG accelerometer worked properly. The external vibration introduced the acceleration change on the inertial mass in the vertical axis, this movement resulted in the stretching or compressing of the FBG. In this way, the external vibration can be measured through the wavelength shift of the FBG[7]. In a realistic experiment, the FBG accelerometer is typically installed in an environment, in which the temperature changes very slowly. In such an environment, the wavelength shift of the FBG is

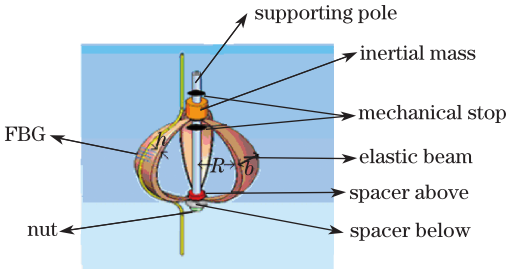

Fig. 1. Schematic diagram of the FBG-based accelerometer.

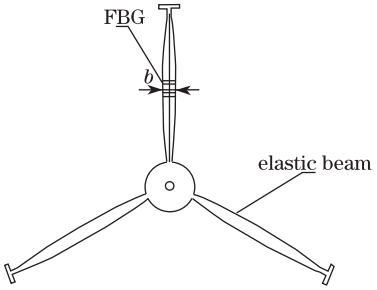

Fig. 2. Expansion graph of the elastic element (flextensional member).

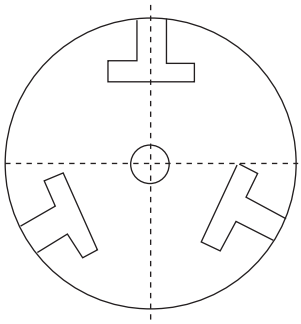

Fig. 3. Schematic diagram of the spacer.

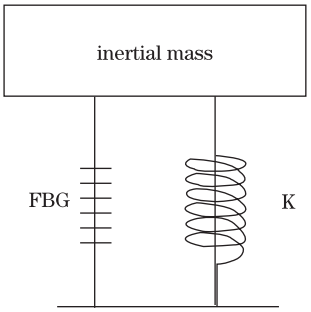

Fig. 4. Mechanical model of the FBG-based accelerometer.

generally affected by temperature. However, in experiment, the vibration frequency was at least dozens of Hertzs. Thus, the wavelength shift of FBG introduced by the temperature can be neglected. The natural frequency and sensitivity of the accelerometer can be tuned by varying the weight of inertial mass. The mechanical model is presented in Fig. 4.

Once the FBG-based accelerometer is subjected to a vertical acceleration, defined as a, the generated force applied to the sensor system is ma, where m is the sum of the inertial mass. Here, $ma/3$ is the reaction force, $maR/3$ is the bending moment, and R is the radius of the curved beam. Stress produced by reaction force can be expressed as

$$\sigma_1 = F/3bh, \tag{1}$$

where h is the thickness of the curved beam, and b is the width of the curved beam. Stress produced by bending moment generates

$$\sigma_2 = maRy/3I_z, \tag{2}$$

where the moment of inertia of the curved beams[8] is $I_z = bh^3/12$, and y is half of the arm thickness.

The strain as a function of equivalent force is described as

$$\varepsilon = (\sigma_2 - \sigma_1)/E = F(12Ry - h^2)/3Ebh^3, \tag{3}$$

where E is the Young's modulus of elastic structure material. According to the basic sensing theory of optical FBG[9], by simple derivation, the shift of the Bragg wavelength as a function of the external acceleration can be expressed as

$$\Delta\lambda_{\rm B} = 0.78\lambda_{\rm B}\varepsilon = \frac{0.78\lambda_{\rm B}m(12Ry - h^2)}{3Ebh^3}a, \tag{4}$$

where $\lambda_{\rm B}$ is the center wavelength of the FBG, and $\Delta\lambda_{\rm B}$ is the shift of the center wavelength.

Equation 5 can only be used if isothermal conditions are considered. Equation (5) indicates that the shift of the Bragg wavelength is linear with external vibration acceleration. External vibration acceleration can be obtained by measuring the change in wavelength. From the above analysis, the wavelength acceleration sensitivity coefficient of the sensor can be defined as

$$S_n = \frac{\Delta\lambda}{a} = \frac{0.78\lambda m(12Ry - h^2)}{3Ebh^3}. \tag{5}$$

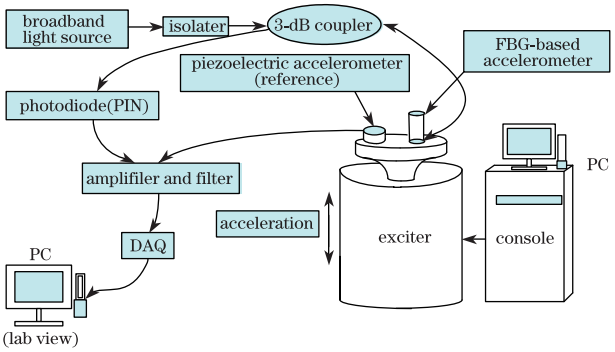

Fig. 5. Schematic diagram of the implemented interrogation system.

From Eqs. (1), (2), and (6), it is known that the sensitivity and natural frequency of the FBG-based accelerometer is related to materials and the geometry size of the flextensional member as well as the mass of m. When the other conditions remain unchanged, the numbers of the arms of the flextensional member is inversely proportional to natural frequency.

The schematic diagram of the implemented interrogation system used to measure dynamic vibrations is presented in Fig. 5. This setup consisted of vibration control system (console), including signal generator, filter circuits, and power amplifier. The exciter was used as the input in the design. The FBG-based accelerometer and a standard piezoelectric accelerometer were fixed on the same exciter actuator to guarantee that their vibrations were the same. The standard piezoelectric accelerometer was used for comparison in the experiment. Input signal was gained by the standard piezoelectric accelerometer, which was used for calibrating the FBG-based accelerometer. In a realistic experiment, this was installed in the environment, in which temperature changed very slowly. In such an environment, the wavelength shift of the FBG is usually impacted by the temperature. However, in our experiment, the vibration frequency was at least dozens of hertzs. Thus, the wavelength shift of the FBG introduced by the temperature can be ignored. The shaker was used in all subsequent tests. A series of dynamic vibration measurements was taken to verify the dynamic characteristic of the FBG-based acceleometer. In the proposed interrogation system, the FBG used in the accelerometer was illuminated by a broadband light source (amplified spontaneous emission source); the light from the light source passed the optical isolator and coupler incident to sensing the FBG. Once it was reflected by the FBG, it became a narrow-band spectrum. Next, it

passed the coupler and reached a photodetector, in which the corresponding electric current signal was formed. The current signal was changed into voltage signal by the current-voltage conversion. Afterwards, the signal passed through the amplifying and filtering circuits and was converted into digital data by a USB-0166 acquisition board (National Instruments) and a data acquisition system before reaching the computer processing system (Labview software). We conducted a series of data processing runs and obtained the final measurement results. The commercial piezoelectric accelerometer was used as a reference, and it was directly injected into the amplifying and filtering circuits. The optical isolator was used to prevent the reflected light of the FBG to affect the stability of the light source.

We set the vibration frequencies for 6 and 10 Hz to detect the frequency response characteristic of the FBG-based accelerometer. The time domain trace and frequency spectra of the output of the FBG-based accelerometer are shown in Figs. 6 and 7, respectively. The tests of different frequencies were carried out by gain control to obtain good waveforms. The FBG-based accelerometer was confirmed to have good frequency detection performance as shown in Figs. 6 and 7.

It is very important for the accelerometer to have a flat response over a range of natural frequency in its practical use. The proposed FBG-based accelerometer and standard piezoelectric accelerometer were installed on the exciter to guarantee that their vibrations were the same. The standard piezoelectric accelerometer was used for reference in the experiments. A continuous sinusoidal signal was produced by the signal generator. The input acceleration value (1 m/s^2) was unchanged in this experiment. The output voltage values of the FBG-based accelerometer were recorded to be within a range of 1–25 Hz as the input frequency scanned continuously. The amplitude–frequency response curve of the FBG-based accelerometer is shown in Fig. 8. The result showed the flat response from 1 to 11 Hz at frequency less than the mechanical resonance frequency (17 Hz), resonance

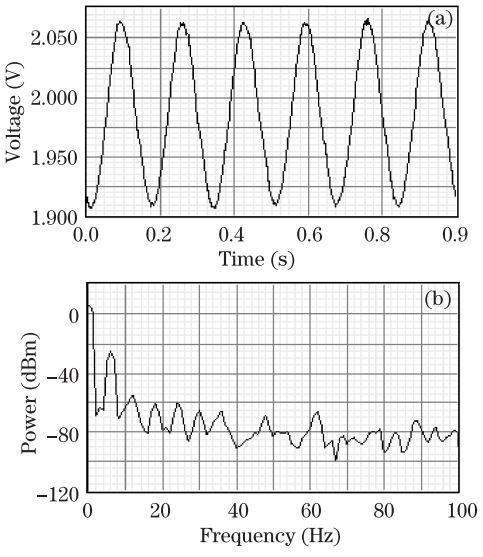

Fig. 6. (a) Time domain trace and (b) frequency spectra of the FBG-based accelerometer with input frequency of 6 Hz.

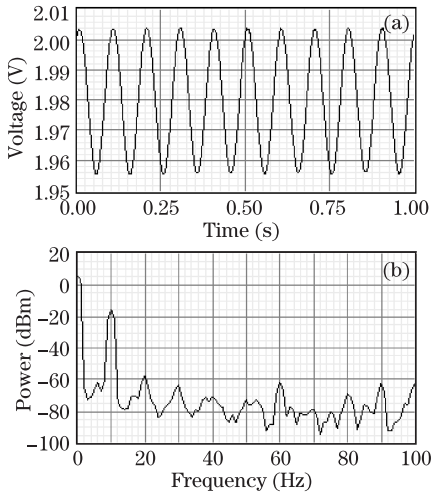

Fig. 7. (a) Time domain trace and (b) frequency spectra of the FBG-based accelerometer with input frequency of 10-Hz output of the FBG-based accelerometer.

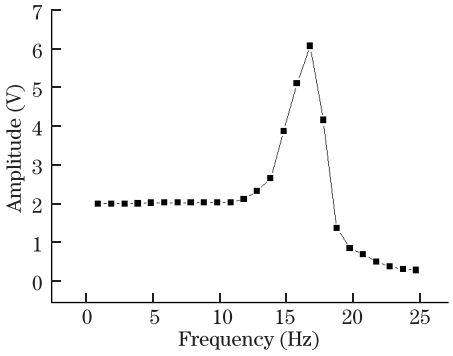

Fig. 8. Amplitude-frequency characteristic curve of the FBG-based accelerometer.

region from 12 to 21 Hz, with the over 21 Hz as the attenuation region. The working region of the FBG-based accelerometer ranged from 1 to 11 Hz.

The free vibration response waveform in the absence of external damping of the FBG accelerator sensor is shown in Fig. 9. The measurement principle is as follows. Firstly, give an initial deflection of the accelerometer by hand; secondly, the hand is removed quickly; finally, we obtain the resulting response waveform. From Fig. 9, we can see that the response waveform of the FBG-based accelerometer is a damped oscillation curve. Through the experimental analytical result, the natural frequency of the sensor (16.7 Hz) was obtained. In practice, we should avoid the vibration frequency, which is close to the natural frequency in order to prevent the resonance that can damage the accelerometer.

The frequency of the input sine wave was 4 Hz, and the acceleration varied from 1 to 5 g. The input acceleration value was obtained from the standard piezoelectric accelerometer; the voltage value was read from the computer with LabView software. The acceleration and output voltage showed a linear relationship; the sensitivity of the FBG accelerometer was 362.3 mV/g, while the linearity was 0.9996 (Fig. 10). The frequency influence on the sensitivity of the FBG accelerometer can be studied in future work.

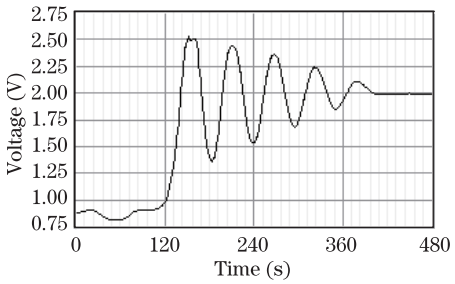

Fig. 9. Free vibration response waveform of the FBG-based accelerometer.

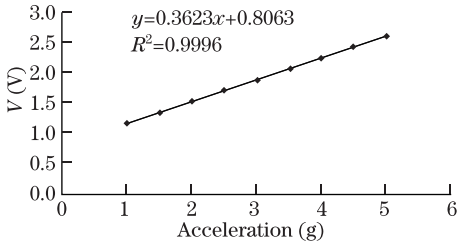

Fig. 10. Sensitivity curve of the FBG-based accelerometer.

In conclusion, a flextensional FBG-based accelerometer is proposed. The dynamic vibration measurements show that it has the following advantages: (i) broad range of flat response (works from 1 to 10 Hz); (ii) high sensitivity (about 410.7 pm/g) with a large measurement range of 0.5 g; (iii) and the natural frequency and sensitivity can be tuned by the addition of the mass. The greatest disadvantages of the FBG accelerometer, however, are its small size under the same sensitivity[10], transverse dimensions is limited under well and beam structure may not be available in measuring within vertical acceleration situations. For structural health monitoring of large-scale engineering structures, an array of the FBG-based accelerometer should be provided[11].

This work was supported by the National Natural Science Foundation of China (Nos. 60727004 and 61077060), the National High Technology Research and Development Program of China (Nos. 2007AA03Z413 and 2009AA06Z203), the International S&T Cooperation Project of MOST of China (No. 2008CR1063), and the Key Scientific and Technological Research Project of Shaanxi Province, China (Nos. 20092KC01-19 and 2008ZDGC-14).

References

1. J.-G. Liu, C. Schmidt-Hattenberger, and G. Borm, Measurement **32,** 151 (2002).
2. A. Cavallo, C. May, A. Minardo, C. Natale, D. Pagliarulo, and S. Pirozzi, Sensors Actuators A **153,** 180 (2009).
3. Y. Zhang, S. Li, Z. Yin, and H.-L. Cui, Proc. SPIE **5796,** 133 (2005).
4. M. J. Bartow, S. G. Calvert, and P. V. Bayly, Proc. SPIE **5278,** 21 (2003).
5. T. Hu, Y. Zhao, X. Li, J. Chen, and Z. Lü, Chin. Opt. Lett. **8,** 392 (2010).
6. T. A. Berkoff and A. D. Kersey, IEEE Photon. Technol. Lett. **8,** 1677 (1996).
7. Y. Zhang, Z. Yin, B. Chen, and H. Cui, Proc. SPIE **5765,** 1112 (2005).
8. E. J. Hearn, *Mechanics of Materials* (Eastbourne, Great Britain, 1997).
9. P. F. C. Antunes, P. A. M. Almeida, and J. L. Pinto, in *Proceedings of Physics Teaching in Engineering Education PTEE 2007* (2007).
10. Z. Luo,"Design and experimental research of fiber Bragg grating low frequency accelerometer" (in Chinese) Master Thesis (Kunming University of Science and Technology, 2008).
11. H. Dong, J. Wu, and G. Zhang, Chin. Opt. Lett. **7,** 23 (2009).